Hypothesis

Transient accumulation of elastic energy in proton translocating ATP synthase

Dmitry A. Cherepanov[a,b], Armen Y. Mulkidjanian[a,c], Wolfgang Junge[a,*]

[a] *Division of Biophysics, Faculty of Biology/Chemistry, University of Osnabrück, D-49069 Osnabrück, Germany*
[b] *A.N. Frumkin Institute of Electrochemistry, Russian Academy of Sciences, Leninskii prosp. 31, 117071 Moscow, Russia*
[c] *A.N. Belozersky Institute of Physico-Chemical Biology, Moscow State University, 119899 Moscow, Russia*

Received 21 January 1999; received in revised form 12 March 1999

Abstract ATP synthase is conceived as a rotatory engine with two reversible drives, the proton-transporting membrane portion, F_0, and the catalytic peripheral portion, F_1. They are mounted on a central shaft (subunit γ) and held together by an eccentric bearing. It is established that the hydrolysis of three molecules of ATP in F_1 drives the shaft over a full circle in three steps of 120° each. Proton flow through F_0 probably generates a 12-stepped rotation of the shaft so that four proton-translocating steps of 30° each drive the synthesis of one molecule of ATP. We addressed the *elasticity* of the transmission between F_0 and F_1 in a model where the four smaller steps in F_0 load a torsional spring which is only released under liberation of ATP from F_1. The kinetic model of an elastic ATP synthase described a wealth of published data on the synthesis/hydrolysis of ATP by F_0F_1 and on proton conduction by F_0 as function of the pH and the protonmotive force. The p*K* values of the proton-carrying group interacting with the acidic and basic sides of the membrane were estimated as 5.3–6.4 and 8.0–8.3, respectively.

Key words: ATP synthase; Elastic energy; Kinetic model

1. Introduction

ATP synthase, F_0F_1, is conceived as a rotatory engine with two reversible drives which are mounted on a central shaft, subunit γ, and linked by an eccentric stator [1–3]. The enzyme either synthesizes ATP at the expense of protonmotive force (PMF), or it generates PMF at the expense of ATP hydrolysis. The same H^+/ATP stoichiometry of 4 has been demonstrated both under static head (quasi-equilibrium between both ends of the enzyme, see [4–6]) and far from equilibrium in kinetic experiments [7]. Three catalytic nucleotide binding sites are arranged with pseudo-C_3 symmetry in the hexagon of subunits $(\alpha\beta)_3$ on F_1. It has been established that the hydrolysis of ATP by isolated F_1 drives the rotation of subunit γ in the middle of the hexagon [8–10] in three steps of 120° each [11–13]. Proton transport in F_0 is supposedly mediated by the 12 copies of the proton binding subunit *c* which are probably arranged as a ring [14,15]. Although the detailed structure of the ring and the nature of partial reactions of proton transfer are under debate, there is agreement that the translocation of one proton drives the ring and the lower portion of γ around by 30° [3,15–17]. After four of those steps, i.e. after a turn of 120°, preformed ATP is eventually extruded from its respective binding site on F_1. This process continues by advancing to the next nucleotide binding site. It has been speculated that F_0 and F_1 are elastically coupled to each other [3,18–20].

We analyzed the *transient elastic storage* of energy derived from four proton-translocation steps until eventual use for the release of the tightly bound ATP. The model of an 'elastic' ATP synthase yielded a fit of kinetic data on F_0F_1 as well as on F_0 with a consistent minimum set of parameters.

2. Elastic tension in ATP synthase

The two-domain structure of ATP synthase with two long α-helical stalks between F_0 and F_1 (see Fig. 1) gives a clue to how the elastic energy storage might function. The proton-translocating rotor portion of F_0 reveals a pseudo-C_{12} symmetry whereas the catalytic headpiece obeys a functional C_3 symmetry. It is conceivable that the intertwined helices of γ serve as a torsional spring and the two parallel α-helices of subunit b_2 [21–23] as a parallelogram-like elastic counterbearing. The latter are topped by subunit δ and probably held together by subunit *a* at the basis (see [3] and references therein). This concept is illustrated in the top part of Fig. 1. The scheme in the bottom part of Fig. 1 symbolizes the stepwise $\Theta_i \rightarrow \Theta_{i+1}$ rotation by 30° of the c_{12} ring relative to the *a* subunit as driven by the sequential proton transfer (see [3,17] for details). It elastically strains F_0F_1 (Fig. 1, middle and bottom) until the elastic energy is large enough to release ATP by stepping the enzyme forward by another 120° in the headpiece. As usual, the total change of free energy per catalytic event, ΔG, is composed of two terms: the free energy change of ATP synthesis $\Delta G_{ATP} = \Delta G^\circ + 2.3RT\log\frac{[ATP]}{[ADP]\cdot[P]}$ and the free energy change derived from the translocation of four protons over the PMF, $\Delta\tilde{\mu}_H = -2.3RT\cdot\Delta pH + F\cdot\Delta\phi$. Considering the four angular positions of the rotor during the sequential transfer of four protons per ATP, one has to involve another term describing the transient storage of elastic energy in the enzyme, $U_n = \sum_{i=1}^{4}\Delta U_i$ where ΔU_i denotes the partial elastic load of the angular transition $\Theta_{i-1} \rightarrow \Theta_i$. The sum U_n is the total elastic load of enzyme in position Θ_n relative to Θ_0.

The elasticity (Young's) module, *E*, is unknown for α-helices, but a figure that has been determined for actin filaments [24], namely 1.8×10^9 N m^{-2}, may serve as a very gross reference. It has been found to be isotropic, i.e. equal in the direc-

*Corresponding author. Fax: (49) (541) 969-1221.
E-mail: junge@uos.de

PII: S0014-5793(99)00386-5

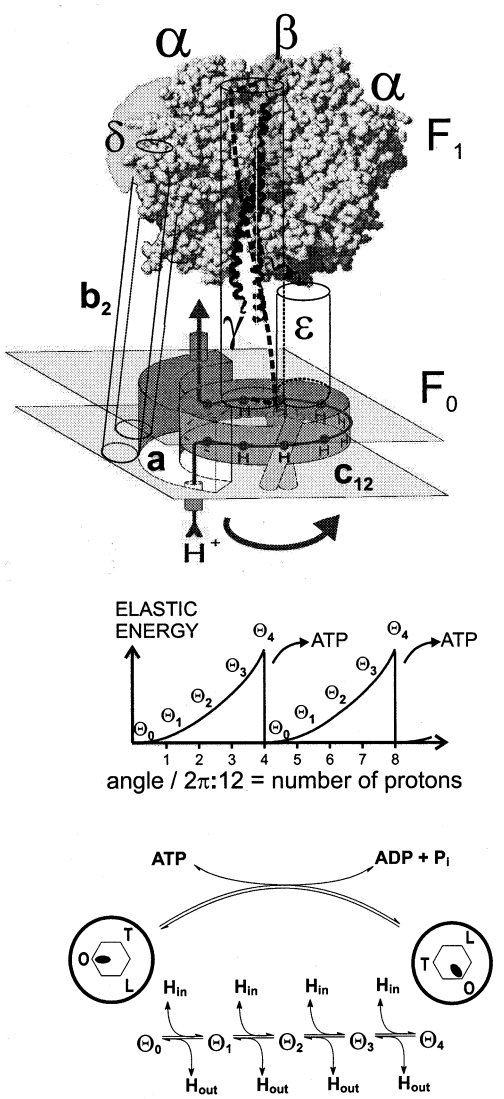

Fig. 1. Schematic illustration of F_0F_1 operation with F_1 elastically coupled to F_0 (adapted from [43]). The topological division into F_0 and F_1 is overlaid by a functional division into rotor (subunits $c_{12}\gamma\varepsilon$) and stator ($ab_2\delta\alpha_3\beta_3$). Twelve proton-carrying copies of subunit *c* are arranged as a ring, the sequential binding of four protons drives the ring four times by 30° to yield 120° and then pushes γ towards the next nucleotide binding site. The two intertwined α-helices of subunit γ might serve as a torsional spring and the two parallel α-helices of b_2 as the elastic counter-bearing to accumulate the energy from these four steps. According to Boyer [2], the catalytic sites on F_1 operate consecutively, circling through three conformational states: the low affinity or 'open' (O) state, where the nucleotides and inorganic phosphate exchange easily between the site and the solution; the medium affinity or 'loose' (L) state, where ADP and P_i exchange more slowly; and the tightly bound (T) state with the highest affinity. In the latter state, the equilibrium between ADP and P_i versus ATP is supposedly poised towards ATP.

tions of twisting, bending, and stretching [25][1]. When subunit γ of F_0F_1 is considered as a solid shaft with radius $R \cong 0.8$ nm and length $L \cong 6$ nm (see the crystal structure [1]), its torsional strain energy is $U = \frac{\pi R^4 E}{8L(1+\sigma)}\theta^2$, where E is Young's longitudinal module, σ is the Poisson ratio (about 0.4 for most elastic materials), and θ is the torsional angle. Using the same figure for Young's module as that of actin, the first step of the angular distortion of γ by $\theta = 30°$ is expected to store a strain energy ΔU_1 of 5 kJ/mol. If the enzyme remains elastic, the strain increases linearly: $\Delta U_2 = 10$, $\Delta U_3 = 15$, and $\Delta U_4 = 20$ kJ/mol during further steps of 30° each. By four successive steps a total energy U_4 of 50 kJ/mol is accumulated. The gross estimate yielded a right order of magnitude to promote ATP synthesis.

3. Modeling the elastic ATP synthase

We analyzed whether the transient storage of elastic energy is consistent with published data on the operation of ATP synthase under steady driving force or, when operating in the reverse, of ATPase. Our kinetic analysis included the following elements: (1) the association-dissociation reactions of protons at the strictly conserved carboxylic residue on the *c* subunit (e.g. Asp-61 in *Escherichia coli* [15]). Its p*K* could differ when accessing the *a*cid and electropositive side of the membrane (A-channel) or the *b*asic negative side (B-channel); (2) the particular ring construct for H^+-translocating ATP synthase, as shown in Fig. 2 and described in [3,17]; (3) the stepwise rotation of the c_{12} oligomer by 30° per translocated proton; (4) the association-dissociation of nucleotide and phosphate at the headpiece; (5) the binding change transitions by 120° in F_1; and (6) the *elastic coupling* between those events. The kinetic properties of the enzyme (see Fig. 1, bottom) depend on whether the binding change transitions in F_1 or the stepwise rotation of the c_{12} oligomer is rate-limiting or not. In the following the latter case is considered. It is physiologically more relevant because the Michaelis constants for ADP and ATP in F_0F_1 are smaller by an order of magnitude than the concentrations of both compounds in the cell. The opposite situation, when ADP and P_i binding is rate-limiting whereas the events in F_0 are in rapid equilibrium, has been treated by Pänke and Rumberg [27]. In this other model the proton concentration in both phases was introduced by only a single parameter, namely the $[H^+]_{in}/[H^+]_{out}$ ratio. The simulated kinetic behavior was thus seemingly independent of pH_{out}, in contrast to experimental data (see below), except for a very narrow domain around the respective pH optimum. In contrast to the former, we focused on the very pH dependence[2].

The kinetic scheme which has been obtained under these simplifying assumptions is shown in Fig. 2. The rate constants of proton delivery/escape to/from the carboxyl of the *c* subunit are k^{on} and k^{off}. Based on experimentally established time constants of proton delivery to a surface-located group at neutral pH and of the protonic equilibration between the surface and the protein interior (both in the range of 10–100 μs [28–30]), we used an estimate $k^{on} = 5 \times 10^{12-pH}$. The respective estimate for the rate constant of proton escape would then be approximated as $k^{off} = 5 \times 10^{12-pK}$. It was assumed that the protolytic reactions are coupled with the angular transitions (at 30° each) of the c_{12} ring, stepping it forward over angular

[1] It is obvious that such a treatment of a protein molecule in terms of Young's module, which is based on continuum mechanics, just serves heuristic purposes. For a recent study on validity and limits of such a treatment see [26].

[2] A merger between both approaches is under way.

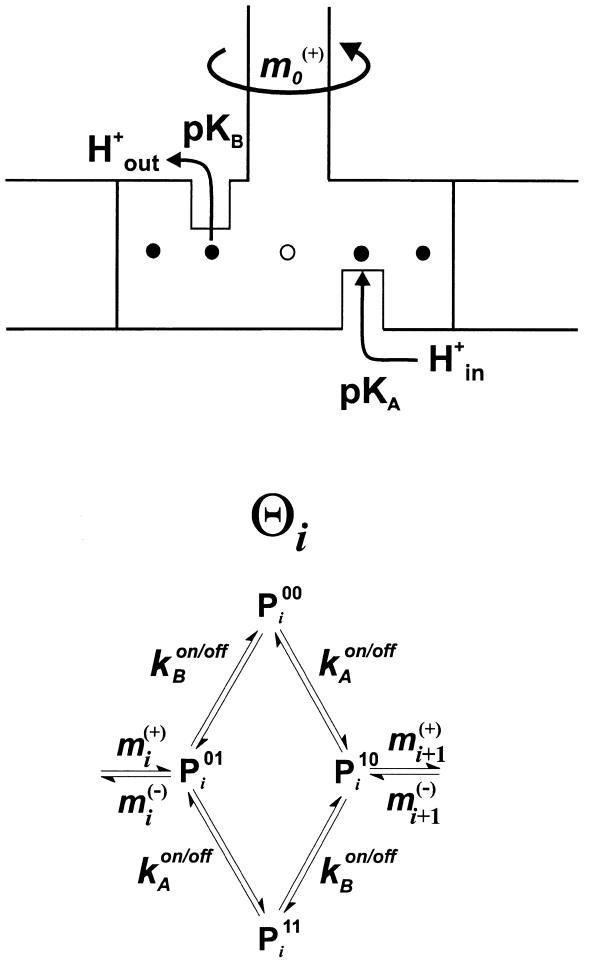

Fig. 2. Kinetic scheme of the elastic coupling between sequential proton transfer reactions in F_0, stepwise $\pm 30°$ rotational transitions of the c_{12} ring, and the catalytic turnover of F_1. The rate constants of proton binding-dissociation reactions k^{on} and k^{off} in the *a*cidic and the *b*asic half-channels are marked by *A* and *B*, respectively; the rate constants $m_i^{(+)}$ and $m_i^{(-)}$ denote the forward and reversed angular transitions (by $\pm 30°$) between configurations Θ_{i-1} and Θ_i. ATP synthesis occurs during the last $\Theta_3 \rightarrow \Theta_4 \Rightarrow \Theta'_0$ transition. The concept of a stochastic rotatory drive based on the ring construct has been outlined in [3] and modeled in [17]. In the latter work it has been emphasized that the construct would not work properly if the back-reaction was not strictly prohibited. Arg-210 on subunit *a* was assumed to electrostatically prevent leakage over the contact zone between the ring of subunit *c* and subunit *a*. This was here taken into account by discarding the possibility of such a back-reaction.

positions Θ_i ($i=0,1,...,4$) before being reset to start the next quadruple of $4\times 30°$ rotatory motion of the ring. The four angular positions $\Theta_1 .. \Theta_4$ are associated with different elastic strains of the enzyme. The rate of rotatory transitions in the synthesis direction is given by $m_i^{(+)}$ and in the reverse (hydrolysis) direction by $m_i^{(-)}$. Without load, the constants $m_i^{(+)}$ and $m_i^{(-)}$ are connected with the pK_A and pK_B values of the proton binding carboxyl group entering the A- and B-side half-channels: $m_i^{(-)}/m_i^{(+)} = 10^{pK_A - pK_B}$. This relation follows from the principle of detailed balance: it prevents any net rotation in the equilibrium. The release of synthesized ATP is assumed to occur during the spontaneous $\Theta_4 \rightarrow \Theta_0$ transition without rotatory motion at the F_0 side of the elastic elements. It removes the strain and resets the system into the initial configuration. The Θ_4 state of one 120° segment is the Θ'_0 state of the following one, except that the state Θ_4 refers to the situation before strain release and Θ'_0 to the one thereafter. For reasons of simplicity and also because of their lower canonic probability, we excluded higher states of greater elastic strain from our consideration. Inasmuch as the elastic energy stored in the enzyme approximately matches the ΔG value of ATP synthesis, the spontaneous reset of the strain may be considered fast compared to the previous stages and we did not consider explicitly the accompanying binding-change transitions.

Whereas the rates of protolytic reactions are independent of Θ_i, the transition rate constants $m_i^{(+)}$ and $m_i^{(-)}$ are altered by the load: $m_i^{(+)} = m_0^{(+)} \cdot 10^{-0.5\Delta U_i}$, $m_i^{(-)} = m_0^{(+)} \cdot 10^{0.5\Delta U_i + pK_A - pK_B}$. The distribution of partial loads ΔU_i depends on the mechanical properties of the F_0F_1 complex. If its behavior is perfectly elastic in a Newtonian way, the stored energy depends linearly on the angular distortion when progressing from Θ_0 to Θ_4: $\Delta U_i = i \cdot \Delta U_1$. Contrastingly, in the absence of a load, when F_1 is removed as in the F_1-depleted F_0, all angular positions Θ_i are supposedly of the same elastic energy.

It is noteworthy that the model has only four fit parameters, namely, the pK_A and pK_B values of carboxyls in the A- and B-channel, the rate constant $m_0^{(+)}$ of the forward angular transition, and the total elastic load $U_4 = 10\Delta U_1$. The steady-state solution of the model wherein the protolytic reactions are explicitly treated is determined by a system of 16 linear equations (i=0, 1, 2, 3):

$$\left\{\begin{array}{c} (k_A^{on} + k_B^{on}) \cdot P_i^{00} - k_B^{off} \cdot P_i^{01} - k_A^{off} \cdot P_i^{10} = 0 \\ k_B^{on} \cdot P_i^{00} - (k_A^{on} + k_B^{off} + m_i^{(-)}) \cdot P_i^{01} + k_A^{off} \cdot P_i^{11} + m_i^{(+)} \cdot P_{i-1}^{10} = 0 \\ k_A^{on} \cdot P_i^{00} - (k_A^{off} + k_B^{on} + m_{i+1}^{(+)}) \cdot P_i^{10} + k_B^{off} \cdot P_i^{11} + m_{i+1}^{(-)} \cdot P_{i+1}^{01} = 0 \\ k_A^{on} \cdot P_i^{01} + k_B^{on} \cdot P_i^{10} - (k_A^{off} + k_B^{off}) \cdot P_i^{11} = 0 \end{array}\right\}$$

Herein P_i^{00}, P_i^{01}, P_i^{10} and P_i^{11} denote the respective probabilities of the four different protonation states of the c_{12} oligomer in the angular position Θ_i. E.g. P_i^{01} refers to a state associated with the angular position Θ_i with the carboxyl in the A-channel unprotonated (first superscript '0') and the one contacting the B-channel protonated (second superscript '1'). Accordingly, $\sum_{i=0}^{3}(P_i^{00} + P_i^{01} + P_i^{10} + P_i^{11}) = 1$. The rate constants of the angular transitions $m_i^{(+)}$ and of the proton binding-dissociation reactions k^{on} and k^{off} were calculated as described above. Under the assumption that the protolytic reactions are fast compared with the angular transitions of the

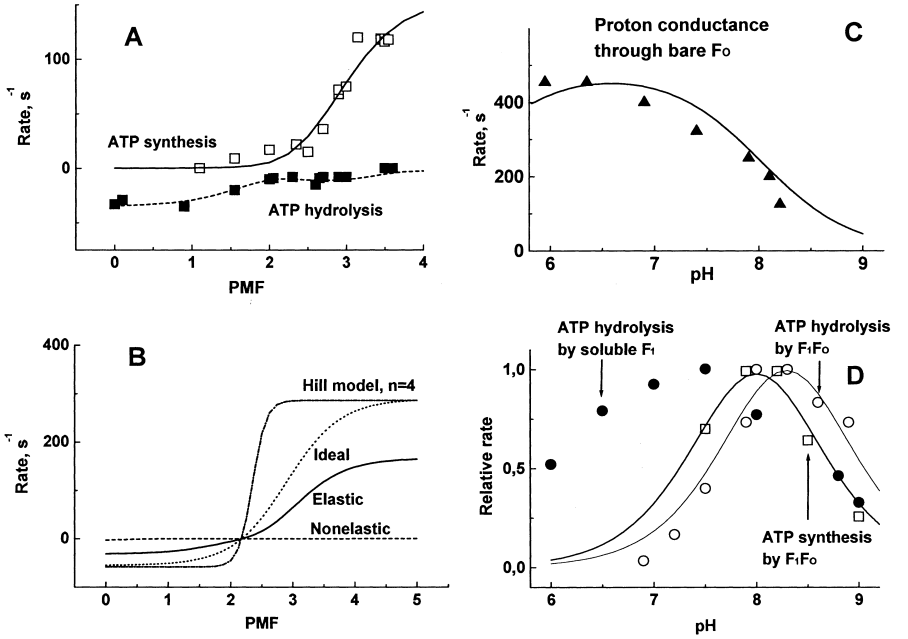

Fig. 3. The performance of the elastically coupled F_0F_1 as a function of PMF and of the pH (points experimental, lines calculated according to the kinetic scheme in Fig. 2, see text). A: The rates of ATP synthesis (open squares) and hydrolysis (solid squares) of spinach ATP synthase at pH 8.2 outside (data from [31]) were fitted with the following set of parameters: $pK_A = 5.3$, $pK_B = 8.0$, $m_0^{(+)} = 2.3\times10^4$ s^{-1}, $\Delta U = 49$ kJ/mol. B: Effect of the elastic load on the calculated proton transfer efficiency of F_0F_1: elastic load distribution (solid curve), the equally distributed partial loads (dotted curve), absence of transient energy storage (dashed curve), the cooperative transfer of four protons (dashed-dotted curve). The same parameter set as in A. C: The broad pH dependence of proton conductance through the F_1-depleted bare F_0 (triangles, data from [42], see also [32]) is described by the same model with zero load (solid curve). The same parameters as in A except $m_0^{(+)} = 2\times10^5$ s^{-1}. D: The sharp pH optimum of ATP synthesis by chloroplast F_0F_1 (open squares, data from [33], re-plotted for ΔpH 3.0. The curve was calculated with the same parameters as in A except $m_0^{(+)} = 2.1\times10^4$ s^{-1}). Coupled ATP hydrolysis in chromatophores of *Rb. sphaeroides* (open circles, data from [35]), the curve was calculated at $pK_A = 6.4$, $pK_B = 8.3$, $m_0^{(+)} = 2.3\times10^4$ s^{-1}, $\Delta U = 49$ kJ/mol, ΔpH 2.0). The filled circles represent the Mg-dependent ATPase activity of isolated spinach F_1 (own data, measured as described in [44]).

c_{12} ring, the number of independent equations reduces to four ($i = 0, 1, 2, 3$):

$$\left\{m_{i+1}^{(+)}\alpha P_i + m_i^{(-)}\beta P_i - m_i^{(+)}\alpha P_{i-1} - m_{i+1}^{(-)}\beta P_{i+1} = 0\right\}$$

Here P_i is the probability of angular position Θ_i, so that $\sum_{i=0}^{3} P_i = 1$, the coefficients α and β account for the proton binding to the c_{12} oligomer:

$$\alpha = \frac{10^{pK_A - pH_A}}{(1 + 10^{pK_A - pH_A})(1 + 10^{pK_B - pH_B})} \text{ and}$$

$$\beta = \frac{10^{pK_B - pH_B}}{(1 + 10^{pK_A - pH_A})(1 + 10^{pK_B - pH_B})}.$$

This simple model described published data on the rates of ATP synthesis *and* hydrolysis by the chloroplast F_0F_1 as a function of the transmembrane pH difference (see Fig. 3A, the experimental points are from Graber et al. [31]) with the following set of four parameters: $pK_A = 5.3$, $pK_B = 8.0$, $m_0^{(+)}$ 2.3×10^4 s^{-1}, $U_4 = 49$ kJ/mol.

It is interesting to analyze the behavior of elastic enzyme near the compensation point. The averaged driving force of the proton transfer, 12.25 kJ/mol, is higher than the elastic energy of the first $\Theta_0 \rightarrow \Theta_1$ transition but is lower than the energy of the last $\Theta_3 \rightarrow \Theta_4$ transition (5.0 and 19.6 kJ/mol, respectively). Consequently, the first step is accompanied by dissipation of the energy while the last one requires 7.1 kJ/mol activation energy. In total, dissipation and activation counterbalance each other and the model is completely reversible at the compensation point.

We checked whether and how the elastic properties of the F_0F_1 complex may improve the catalytic performance of enzyme. Fig. 3B compares the calculated elastic behavior from Fig. 3A (continuous line) with a non-elastic behavior without transient energy storage, when the whole load is centered at the last step ($\Delta U_1 = 0$, $\Delta U_2 = 0$, $\Delta U_3 = 0$, $\Delta U_4 = \Delta U$, dashed curve). Not unexpectedly, both ATP synthesis and ATP hydrolysis were practically blocked in the absence of elasticity. From the standpoint of efficiency, the 'elastic' ATP synthase operated only two times less effectively as compared with the ideal, but physically unrealistic case of equally distributed loads (dotted line). For comparison, the dashed-dotted line shows the behavior of the enzyme where four protons are transferred cooperatively (calculated by the phenomenological Hill equation with $n = 4$). The slope of this curve is much steeper than the observed one (compare Fig. 3A).

The rate of proton conduction by the bare F_0 is weakly pH-dependent (see [32] and Fig. 3C). The pH dependence of ATP hydrolysis by *isolated* F_1 is also rather broad (closed circles in Fig. 3D, own data). The coupled chloroplast F_0F_1, however, reveals a sharp pH optimum at pH about 8 (see open squares in Fig. 3D, data from [33]). The sharpness of the pH dependence of ATP synthesis could not be attributed to the pH dependence of the catalytic F_1 portion in the whole F_0F_1, as the rate of ATP synthesis, driven by saturating high membrane potential, was independent of the pH_{out} in the pH range

from 7 to 9 [34]. As shown in Fig. 3C,D, the 'elastic' enzyme model described the rather different pH dependences of proton flow through the coupled F_0F_1 ($U_4 = 49$ kJ/mol) and through the 'bare' F_0 ($U_4 = 0$) with same values of pK_A and pK_B as in Fig. 3A. The pK values obtained here for the chloroplast F_0F_1 using the elastic model are close to those resulting from an analysis by the phenomenological Hill equation (5.3 and 7.8, respectively) as carried out by Possmayer and Gräber [33]. The open circles in Fig. 3D show the pH dependence of the coupled ATP hydrolysis in chromatophores of *Rhodobacter sphaeroides* (data from [35]). A fit by the elastic model yielded $pK_A = 6.4$ and $pK_B = 8.3$ and the same values of $m_0^{(+)}$ and U_4 as in Fig. 3A. It is noteworthy that both pK values are shifted somewhat into the basic pH range as compared with the chloroplast F_0F_1.

4. Functional implications

The difference between $pK_A \sim 5.5$ and $pK_B \sim 8.0$ may be functionally relevant. When the pH is neutral at both sides of the membrane, the protonic conductivity of F_0F_1 in the synthesis direction is low owing to the small probability of the protonation inside ($pK_A < pH$) and of the deprotonation outside ($pK_B > pH$). This accounts for the weak pH dependence of the proton conductivity via a bare F_0 at $pK_A < pH < pK_B$ (Fig. 3C). When $\Delta\tilde{\mu}_H$ approaches the apparent 'threshold value' for ATP synthesis by F_0F_1 (about 2.5 pH units, acid inside), the proton transfer in the 'synthesis' direction becomes more effective with a rather sharp maximum at $pH \sim pK_B$ (Fig. 3D, open squares). During the hydrolysis-driven proton pumping at neutral pH the proton-carrying group can easily trap proton from the basic side of membrane ($pK_B > pH$) and the mechanical transition of the protonated group into the channel A (by the ATP-driven 'hydrolytic' rotation of the γ subunit) will result in the spontaneous proton release at the other side ($pK_A < pH$).

The elastic operation of ATP synthase implies a stepwise loading of the enzyme before ATP synthesis can occur. This may account for the wealth of phenomena attributed to the 'activation' transitions both in F_0 (see [36] and references therein) and in F_1 (reviewed in [37]). It is noteworthy that a winding up by 120° of a shaft with the elastic properties and the length of the γ subunit will cause its shortening by ~ 10 Å. This may cause some of the reported conformational changes in ε and γ subunits upon energization (see [38] for review). Furthermore, the statistical distribution of states Θ_0–Θ_4 in elastic F_0F_1 depends on the magnitude of the PMF. Under conditions of ATP synthesis, the higher states Θ_3 and Θ_4 are expected to dominate (the transfer of the fourth proton during $\Theta_3 \rightarrow \Theta_4$ is rate-limiting). During hydrolysis, the probability of lower states is higher (the elastic driving force for $\Theta_1 \rightarrow \Theta_0$ transition is, apparently, less than $\Delta\tilde{\mu}_H$). Thus, the averaged elastic state during the turnover of ATP synthase is expected to differ from that of ATPase. This may account for the functional non-equivalence between these two forms of the enzyme as claimed in the literature [39–41].

In conclusion, the presented theoretical considerations favor the view that ATP synthase stepwise *accumulates* energy from the transmembrane potential difference of protons (or sodium ions in the Na^+-translocating ATP synthase) and transiently stores it as elastic strain in the protein. The transmission between a 12-stepped and a three-stepped portions of this enzyme requires, perhaps, more highly developed elastic constructs than present in other mechanoenzymes. Hence, ATP synthase with its unique *electro-mechano-chemical* function is becoming a simplex model to study molecular mechanics. It is a major challenge to read out the elastic deformations by spectroscopic techniques.

Acknowledgements: This work was financially supported by the Deutsche Forschungsgemeinschaft (SFB 171-B3, SFB 431-D1, DFG-RUS-436, Mu-1285/1) and by the Fonds der Chemischen Industrie. Additional support from the EU Commission (INTAS-93-2852) is greatly appreciated.

References

[1] Abrahams, J.P., Leslie, A.G.W., Lutter, R. and Walker, J. (1994) Nature 370, 621–628.
[2] Boyer, P. (1997) Annu. Rev. Biochem. 66, 717–749.
[3] Junge, W., Lill, H. and Engelbrecht, S. (1997) Trends Biochem. Sci. 22, 420–423.
[4] van Walraven, H.S., Strotmann, H., Schwarz, O. and Rumberg, B. (1996) FEBS Lett. 379, 309–313.
[5] Pitard, B., Richard, P., Dunach, M. and Rigaud, J.L. (1996) Eur. J. Biochem. 235, 779–788.
[6] Berry, S. and Rumberg, B. (1996) Biochim. Biophys. Acta 1276, 51–56.
[7] Pänke, O. and Rumberg, B. (1997) Biochim. Biophys. Acta 1322, 183–194.
[8] Duncan, T.M., Bulygin, V.V., Zhou, Y., Hutcheon, M.L. and Cross, R.L. (1995) Proc. Natl. Acad. Sci. USA 92, 10964–10968.
[9] Sabbert, D., Engelbrecht, S. and Junge, W. (1996) Nature 381, 623–626.
[10] Noji, H., Yasuda, R., Yoshida, M. and Kinosita, K. (1997) Nature 386, 299–302.
[11] Sabbert, D. and Junge, W. (1997) Proc. Natl. Acad. Sci. USA 94, 2312–2317.
[12] Häsler, K., Engelbrecht, S. and Junge, W. (1998) FEBS Lett. 426, 301–304.
[13] Yasuda, R., Noji, H., Kinosita Jr., K. and Yoshida, M. (1998) Cell 93, 1117–1124.
[14] Singh, S., Turina, P., Bustamante, C.J., Keller, D.J. and Capaldi, R. (1996) FEBS Lett. 397, 30–44.
[15] Fillingame, R.H., Jones, P.C., Jiang, W., Valiyaveetil, F.I. and Dmitriev, O.Y. (1998) Biochim. Biophys. Acta 1365, 135–142.
[16] Dimroth, P., Kaim, G. and Matthey, U. (1998) Biochim. Biophys. Acta 1365, 87–92.
[17] Elston, T., Wang, H. and Oster, G. (1998) Nature 391, 510–513.
[18] Kagawa, Y. and Hamamoto, T. (1996) J. Bioenerg. Biomembr. 28, 421–431.
[19] Pänke, O. and Rumberg, B. (1996) FEBS Lett. 383, 196–200.
[20] Wang, H. and Oster, G. (1998) Nature 396, 279–282.
[21] Rodgers, A.J., Wilkens, S., Aggeler, R., Morris, M.B., Howitt, S.M. and Capaldi, R.A. (1997) J. Biol. Chem. 272, 31058–31064.
[22] Dunn, S.D. and Chandler, J. (1998) J. Biol. Chem. 273, 8646–8651.
[23] Wilkens, S. and Capaldi, R.A. (1998) Nature 393, 29.
[24] Kojima, H., Ishijima, A. and Yanagida, T. (1994) Proc. Natl. Acad. Sci. USA 91, 12962–12966.
[25] Tsuda, Y., Yasutake, H., Ishijima, A. and Yanagida, T. (1996) Proc. Natl. Acad. Sci. USA 93, 12937–12942.
[26] Oberhauser, A.F., Marszalek, P.E., Erickson, H.P. and Fernandez, J.M. (1998) Nature 393, 181–185.
[27] Pänke, O. and Rumberg, B. (1998) in: Photosynthesis: Mechanisms and Effects (Garab, G., Ed.), Kluwer Academic, Dordrecht.
[28] Heberle, J., Riesle, J., Thiedemann, G., Oesterhelt, D. and Dencher, N.A. (1994) Nature 370, 379–382.
[29] Marantz, Y., Nachliel, E., Aagaard, A., Brzezinski, P. and Gutman, M. (1998) Proc. Natl. Acad. Sci. USA 95, 8590–8595.
[30] Gopta, O.A., Cherepanov, D.A., Junge, W. and Mulkidjanian, A.Y. (1998) in: Photosynthesis: Mechanisms and Effects (Garab, G., Ed.), Kluwer Academic, Dordrecht.

[31] Graber, P., Junesch, U. and Thulke G. (1987) in: Progress in Photosynthesis Research (Biggens, J., Ed.), Vol. III, pp. 177–184, Martinus Nijhoff, Dordrecht.
[32] Althoff, G., Lill, H. and Junge, W. (1987) J. Membr. Biol. 108, 263–271.
[33] Possmayer, F.E. and Gräber, P. (1994) J. Biol. Chem. 269, 1896–1904.
[34] Schlodder, E., Gräber, P. and Witt, H.T. (1982) in: Electron Transfer and Phosphorylation (Barber, J., Ed.), pp. 107–175, Elsevier, Amsterdam.
[35] Reed, D.W. and Raveed, D. (1972) Biochim. Biophys. Acta 283, 79–91.
[36] Groth, G. and Junge, W. (1995) Biochemistry 34, 8589–8596.
[37] Mills, J.D. (1996) in: Oxygenic Photosynthesis: The Light Reactions (Ort, D.R. and Yocum, C.F., Eds.), pp. 469–485, Kluwer Academic, Dordrecht.
[38] Richter, M.L. and Gao, F. (1996) J. Bioenerg. Biomembr. 28, 443–449.
[39] Syroeshkin, A.V., Vasilyeva, E.A. and Vinogradov, A.D. (1995) FEBS Lett. 366, 29–32.
[40] Bald, D., Amano, T., Muneyuki, E., Pitard, B., Rigaud, J.L., Kruip, J., Hisabori, T., Yoshida, M. and Shibata, M. (1998) J. Biol. Chem. 273, 865–870.
[41] Syroeshkin, A.V., Bakeeva, L.E. and Cherepanov, A.D. (1999) Biochim. Biophys. Acta 1409, 59–71.
[42] Althoff, G. (1991) Der Protonenkanal der F-ATPase aus Chloroplasten, Ph.D. Thesis, Universität Osnabrück.
[43] Engelbrecht, S. and Junge, W. (1997) FEBS Lett. 414, 485–491.
[44] Schulenberg, B., Wellmer, F., Lill, H., Junge, W. and Engelbrecht, S. (1997) Eur. J. Biochem. 249, 134–141.